Journal of Sound and Vibration (1999) **227**(4), 749–768
Article No. jsvi.1999.2347, available online at http://www.idealibrary.com on IDEAL®

RITZ-TYPE DYNAMIC ANALYSIS OF CROSS-PLY LAMINATED CIRCULAR CYLINDERS SUBJECTED TO DIFFERENT BOUNDARY CONDITIONS

A. MESSINA

Dipartimento di Scienza dei Materiali, Università di Lecce, 73100 Lecce, Italy

AND

K. P. SOLDATOS

University of Nottingham, Pope Building, Nottingham NG7 2RD, England

(*Received* 5 *January* 1999, *and in final form* 5 *May* 1999)

This paper extends the applicability of the Ritz-type method presented in a previous publication [1] towards an advanced study of the influence of the edge boundary conditions on the vibration characteristics of complete, cross-ply laminated cylindrical shells. The analysis is based on a combination of the Ritz method with appropriate, complete bases of orthonormal polynomials and its subsequent application on the energy functional of the love-type version of a unified shear-deformable shell theory. As a result, two different kinds of shear deformable Love-type shell theories are employed, including versions that either fulfil or violate the continuity of the interlaminar stresses through the shell thickness. Apart from the study of the physical problem itself, several features related to the theoretical model as well as to the analytical procedure are further addressed and investigated. As far as the modelling is concerned, particular emphasis is given to the version of the parabolic shear deformable shell theory that considers continuity of interlaminar stresses. Moreover, the relation of this version of the theory as well as its performance with respect to the corresponding older version that violates this continuity requirement [8] is further investigated. It is concluded that the accurate modelling of the interlaminar stress distribution may become a serious issue for further investigation, as it already is for the stress analysis of laminated composite structural elements.

1. INTRODUCTION

A recent paper [1] initiated a study of the free vibration characteristics of transverse shear deformable cross-ply laminated circular cylindrical shells on the basic of the Ritz method. The analysis was based on the energy functional of the Love-type version of the unified shell theory present in reference [2]. As a result, several kinds of shear deformable Love-type shell theories were employed, along with their classical counterpart, and a version that accounts for continuity of the

0022-460X/99/440749 + 20 $30.00/0

interlaminar stresses was found to be a particular interest. The Ritz-type theoretical formulation was given in a general form but the variational approach was finally applied in conjunction with a complete functional basic made up of the appropriate admissible orthogonal polynomials. Despite that the method is capable of treating cross-ply laminated circular cylindrical shells subject to any set of variationally consistent edge boundary conditions, particular emphasis was given to the free vibrations of shells having one or both of their edges free of external tractions.

The particular interest in the dynamic investigation of cylinders having one or both of their edges free of external tractions is merely due to the fact that such structural elements are very common in engineering applications and relatively easy to achieve in a laboratory. The case of completely free shells, in particular, constitutes a privileged class of structural elements for laboratory tests and, in this respect, some of the relevant analytical results obtained in reference [1] were found to be in a good agreement with corresponding experimental frequencies [3]. Moreover, the features and the efficiency of the proposed Ritz-type analysis were exhibited by comparing its results with the very few existing relevant results obtained, elsewhere [4, 5], on the basis of the state space concept. These comparisons showed a fast convergence of the method towards the exact frequency values, regardless of the shell theory employed. It was also concluded that orthonormal rather than simply orthogonal polynomial bases should be preferred, particularly when higher vibration frequencies and mode shapes are sought.

Apart from the specific value of the dynamic investigation presented in reference [1], its analysis was further considered as a successful test towards its extension for the study of corresponding problems in which the state space concept cannot be applied directly. Hence, the one-dimensional Ritz-type procedure has already been extended to two dimensions towards the successful dynamic analysis of cross-ply laminated plates and open cylindrical panels having all their four edge free of traction [6] or being subjected to different sets of edge boundary conditions [7]. However, there is still a considerable lack of corresponding information dealing with the dynamic analysis of cross-ply laminated, shear deformable, complete cylindrical shells subjected to different sets of edge boundary conditions.

In an attempt to fill the described lack of relevant information, this paper extends the applicability of the Ritz-type method presented in reference [1] towards a study of the influence of the edge boundary conditions on the vibration characteristics of complete cross-ply laminated cylindrical shells. However apart from the study of the physical problem itself, several features related to the theoretical model as well as to the analytical procedure are further addressed and investigated. As far as the modelling is concerned, particular emphasis is given to the version of the parabolic shear deformable shell theory that considers continuity of interlaminar stresses [1, 2, 5]. Moreover, the relation of this version of the theory as well as its performance with respect to the corresponding older version that violates this continuity of requirement [8] is further investigated. As far as the Ritz-type procedure is concerned, further convergence tests are carried out in an attempt to estimate the efficiency of the method when different sets of boundary conditions are applied on the shell edges. It should be mentioned that the presentation of the mathematical model employed in this paper is described in reference [1]. Hence,

apart from some principal relevant features which are outlined in the next section for the sake of self-consistency, the main contribution of the present study is related to the mechanics of the dynamic problem considered and to the corresponding interpretations revealed through the numerical results presented or the subsequent discussion.

2. THEORETICAL FORMULATION

Consider a circular cylindrical shell having a constant thickness h, an axial length L_x, and a middle-surface radius R (Figure 1). The axial, circumferential and normal to the middle surface-coordinate length parameters are denoted with x, s and z, respectively, whereas U, V and W represent the corresponding displacement components. In accordance with the definition of a cross-ply material arrangement [9], the shell is made up of an arbitrary number, L, of linearly elastic orthotropic layers, the material axes of which coincide with the axes of the adopted curvilinear co-ordinate system. Hence, under the usual thin shell theory assumption of negligible transverse normal strains, the stress–strain relationships in the kth layer (starting counting from the bottom layer) are given as follows ($k = 1, 2, \ldots, L$):

$$\begin{bmatrix} \sigma_x^{(k)} \\ \sigma_s^{(k)} \\ \tau_{xs}^{(k)} \end{bmatrix} = \begin{bmatrix} Q_{11}^{(k)} & Q_{12}^{(k)} & 0 \\ Q_{12}^{(k)} & Q_{22}^{(k)} & 0 \\ 0 & 0 & Q_{66}^{(k)} \end{bmatrix} \begin{bmatrix} \varepsilon_x \\ \varepsilon_s \\ \gamma_{xs} \end{bmatrix}, \quad \begin{bmatrix} \tau_{sz}^{(kk)} \\ \tau_{xz}^{(k)} \end{bmatrix} = \begin{bmatrix} Q_{44}^{k} & 0 \\ 0 & Q_{55}^{(k)} \end{bmatrix} \begin{bmatrix} \gamma_{sz} \\ \gamma_{xz} \end{bmatrix}, \tag{1}$$

where the appearing reduced stiffness are defined in reference [9].

The shell-type approximations employed in this study are consistent with the general, shear deformable, Love-type shell theory, the main features and basic

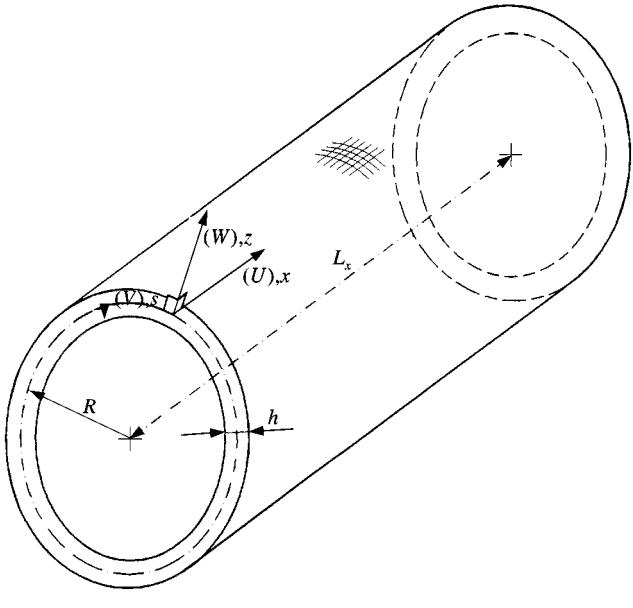

Figure 1. Nomenclature and co-ordinate system of the laminated circular cylinder.

equations of which are detailed in references [1, 2, 5]. It should be further specified, however, that two versions of the parabolic shear deformable shell theory will be employed for the purpose of the present study, together with their classical shell theory counterpart. One version (PAR_{ds}) is based on the following choice of the functions that dictate the through thickness distribution of transverse shear strains:

$$\Phi_1(z) = \Phi_2(z) = z\,(1 - 4z^2/3h^2), \tag{2}$$

and, as a result, it is equivalent with the corresponding theory that violates the continuity requirement of the interlaminar stresses [8]. The main model of interest in this investigation is, however, a second version of the theory (PAR_{cs}), which is based on the corresponding shape functions developed in reference [7] and can therefore account for the continuity of interlaminar stresses. It should be noted, however, that both PAR_{ds} and PAR_{cs} coincide in the case of a homogenous shell, in which material interfaces are not present. The classical shell theory (CST) counterpart of both version of the shear deformable theory employed is obtained by nullifying both of the afore-mentioned shape functions.

In accordance with the Ritz-type analysis followed in reference [1], the five unknown displacement functions of the shear deformable model employed are expressed in the following form:

$$\begin{aligned}
u(x, s; t) &= \cos(\omega t)\sin(ns/R)\sum_{m=1}^{M} A_m X_m^u(x),\\
v(x, s; t) &= \cos(\omega t)\cos(ns/R)\sum_{m=1}^{M} B_m X_m^v(x),\\
w(x, s; t) &= \cos(\omega t)\sin(ns/R)\sum_{m=1}^{M} C_m X_m^w(x),\\
u_1(x, s; t) &= \cos(\omega t)\sin(ns/R)\sum_{m=1}^{M} D_m X_m^{ul}(x),\\
v_1(x, s; t) &= \cos(\omega t)\cos(ns/R)\sum_{m=1}^{M} E_m X_m^{vl}(x),
\end{aligned} \tag{3}$$

where t is the time, ω is an unknown natural frequency of vibration and the non-negative integer n represents the circumferential wave number of the corresponding mode shape. The standard s-dependent parts in these representations enable the satisfaction of all the periodicity requirements that should hold around the circumference of a closed cylindrical shell. In the present form of equations, the $n = 0$ choice represents the torsional vibration pattern of the cylindrical shell considered. The corresponding axisymmetric (longitudinal) vibration pattern is chosen by keeping $n = 0$ but by replacing the appearing sin and cos functions with cos and sin respectively.

Each of the summation appearing in equations (3), represents a series expansion of the unknown x-dependent part of the corresponding displacement function. The set of the appearing basis functions employed in this paper are orthonormal polynomials [10, 11] that satisfy all the geometric boundary conditions applied on

the shell edges ($x = 0, L_x$). In more detail, given the first orthogonal polynomial, $\psi_1(x)$, the remaining members of such a complete functional basic are constructed according to the following recursive formulas [10]:

$$\psi_2(x) = (x - B_2)\,\psi_1(x),$$

$$\psi_k(x) = (x - B_k)\,\psi_{k-1}(x) - C_k\,\psi_{k-2}(x), \quad \textit{for } k > 2,$$

$$B_k = \frac{\int_0^{Lx} x\psi_{k-1}^2(x)\,\mathrm{d}x}{\int_0^{Lx} \psi_{k-1}^2(x)\,\mathrm{d}x}, \quad C_k = \frac{\int_0^{Lx} x\psi_{k-1}(x)\,\psi_{k-2}(x)\mathrm{d}x}{\int_0^{Lx} \psi_{k-2}^2(x)\,\mathrm{d}x} \tag{4}$$

Upon further dividing each one of its members by the square root of the norm:

$$\| \psi_k(x) \| = \int_0^L \psi_k^2(x)\,\mathrm{d}x, \tag{5}$$

the complete orthogonal polynomial basic thus developed is converted into a corresponding orthonormal one.

The numerical results presented and discussed in the next section are for cylindrical shells the edges of which are subjected to all six possible combinations of certain simply supported, clamped and free boundary conditions. In more detail, cylindrical shells having both their edges clamped, simply supported or free of tractions will be referred to as CC, SS and FF shells, respectively. Similarly, shells having one edge clamped and the other either simply supported or free of tractions will be referred to as CS shells or CF shells, respectively, whereas shells having one edge simply supported and the other free of tractions will be referred to as SF shells. In each of these cases, the geometrical conditions satisfied by all the members of the afore-mentioned orthonormal polynomial basis, as well as the first polynomial needed in the recursive formulas (4) for the construction of that basis, are given in Table 1.

The $5M$ unknown coefficients ($3M$ in the case of a CST) that appear in equations (3) are determined by solving the generalized algebraic eigenvalue problem of the form

$$(\mathbf{K} - \omega^2\,\mathbf{M})\,\mathbf{X} = \mathbf{0}, \tag{6}$$

which is obtained by looking for the stationary values of the Hamiltonian of the cylindrical shell considered (Ritz method). Details regarding the form of the elements of the appearing $5M \times 5M$ stiffness, $\mathbf{K}$, and inertia, $\mathbf{M}$, matrices ($3M \times 3M$ in the case of a CST) are given in reference [1]. It might useful to note here that, in the $n = 0$ case, the dimension of the $\mathbf{K}$ and $\mathbf{M}$ matrices is $2M$ if torsional vibrations are sought whereas is $3M$ if longitudinal vibrations are studied. Due to the completeness of the orthonormal polynomial bases employed in the corresponding functional (Hilbert) space, the series expansions (3) determined after the successful solution of the eigenvalue problem (6), approaches (asymptotically) the unique solution of the dynamical problem considered as M approaches infinity.

TABLE 1

Sets of boundary conditions employed and first polynomial terms that generate the orthogonal basis in the corresponding functions (Hilbert) space ($\xi = x/L_x$)

B.C. set	Essential conditions	First polynomial
CC	$x = 0$: $u = v = w = u_1 = v_1 = 0$; $dw/dx = 0$; $x = L_x$: $u = v = w = u_1 = v_1 = 0$; $dw/dx = 0$;	$\alpha = (w)$: $X_1^\alpha(\xi) = 3\,\xi^4 - 6\,\xi^3 + 3\,\xi^2$; $\alpha = (u; v; u_1; v_1)$: $X_1^\alpha(\xi) = \xi^2 - \xi$;
SS	$x = 0$: $v = w = v_1 = 0$; $x = L_x$: $v = w = v_1 = 0$;	$\alpha = (v; w; v_1)$: $X_1^\alpha(\xi) = \xi^2 - \xi$; $\alpha = (u; u_1)$: $X_1^\alpha(\xi) = 1$;
FF	$x = 0$: No constraints; $x = L_x$: No constraints;	$\alpha = (u; v; w; u_1; v_1)$: $X_1^\alpha(\xi) = 1$;
CS	$x = 0$: $u = v = w = u_1 = v_1 = 0$; $dw/dx = 0$; $x = L_x$: $v = w = v_1 = 0$;	$\alpha = (u; u_1)$: $X_1^\alpha(\xi) = \xi$; $\alpha = (v; v_1)$: $X_1^\alpha(\xi) = \xi^2 - \xi$; $\alpha = (w)$: $X_1^\alpha(\xi) = \xi^3 - \xi^2$;
CF	$x = 0$: $u = v = w = u_1 = v_1 = 0$; $dw/dx = 0$; $x = L_x$: No constraints	$\alpha = (u; v; u_1; v_1)$: $X_1^\alpha(\xi) = \xi$; $\alpha = (w)$: $X_1^\alpha(\xi) = \xi^2$;
SF	$x = 0$: $v = w = v_1 = 0$; $x = L_x$: No constraints;	$\alpha = (v; w; v_1)$; $X_1^\alpha(\xi) = \xi$; $\alpha = (u; u_1)$; $X_1^\alpha(\xi) = 1$;

3. NUMERICAL EXAMPLES AND DISCUSSION

In order to check the reliability of the method, some successful comparisons were initially performed in reference [1] with corresponding numerical results obtained in reference [4, 5] on the basic of the state space concept. Since, however, reference [1] dealt with certain cylinders having at least one of their curved edges free, these comparisons were for open cylindrical panels having both their straight edges simply supported and their curved edges free of external tractions [4] or for cantilevered complete shells [5]. In the present paper, in which the barrier of the edge boundary conditions is removed, the results of some further relevant comparisons and convergence tests are initially performed in Tables 2–4 before further new results are presented and discussed. It has to be emphasized, however, that, despite the relatively large number of different sets of boundary conditions considered in this paper, there exist very limited relevant numerical results that are based on alternative mathematical methods [12] or models [13].

For certain types of two- and four-layered SS and CC shells, Table 2 compares the fundamental frequency parameters,

$$\omega^* = \omega R \sqrt{\rho/E_2}, \tag{7}$$

obtained on the basis of the present approach with the corresponding parameters presented in reference [12]. Reference [12] was based on an CST model only, but it dealt with the free vibration of angle-ply laminated cylindrical shells, the material

TABLE 2

Comparison of frequency parameters, ω^*, for different wave numbers and polynomial terms ($L_x/R = 2$; $h/R = 0.0025$)

Boundary conditions	Stacking sequence	Reference [12]	Full wave numbers	Present: CST M		
				4	8	14
SS	[90°/0°]	0·1246	8	0·12464	0·12462	0·12462
	[0°/90°{	0·1200	8	0·12004	0·12003	0·12003
	[0°/90°/0°/90°]	0·1412	7	0·14125	0·14124	0·14124
	[90°/0°/90°/0°]	0·1431	7	0·14306	0·14305	0·14305
	[0°/90°/90°/0°]	0·1170	8	0·11700	0·11698	0·11698
	[90°/0°/0°/90°]	0·1649	6	0·16489	0·16487	0·16487
CC	[90°/0°]	0·1535	8	0·15826	0·15351	0·15274
	[0°/90°]	0·1517	8	0·15620	0·15174	0·15096

arrangement of which contains the present cross-ply arrangement as a particular case. Since CST approximations were only used in reference [12], all of the present results obtained for the comparisons performed in Table 2 were similarly based on the CST version of the present model. In this respect, the following material properties that were used in reference [12]:

$$E_1 = 15{\cdot}59E_2, \quad G_{12} = 0{\cdot}5366E_2, \quad \nu_{12} = 0{\cdot}32, \tag{8}$$

are still adequate for all the numerical results presented in Table 2.

The approach followed in reference [12] was based on the combination of the Ritz method with double series expansions of the three unknown displacement components. In more detail, simple powers of the x co-ordinate parameter were essentially used in the x-part of those series expansions, the s-part of which made use of certain trigonometric functions, similar to those employed in equations (3). Upon setting a maximum, fixed, number for the circumferential terms involved, that way [12] of tackling the problem prevents the use of n as an external data parameter whereas it enables the ordering of the natural frequency parameters in an ascending order. As is known on the other hand (see for instance references [14, 15]), every single value of n represents a single vibration harmonic which, either for cross- or for angle-ply laminated circular cylinders, is "circumferentially" uncoupled from the remaining ones. Hence, as far as the present case of cross-ply laminates is concerned, the single-series expansions used in equations (3) are "circumferentially" equivalent to those employed in reference [12]. As far as the numerical solutions of the eigenvalue problem (6) is concerned, however, the present series expansions are more economical. Under these considerations, Table 2 also gives the value of n for which a fundamental frequency was detected, a piece of information that is missing in reference [12]. Moreover, unlike reference [12] that made use of a fixed value of terms in the axial series expansion ($M = 8$),

TABLE 3

Comparison of frequency parameters, $\hat{\omega}$, for different wave numbers and polynomial terms for isotropic FF cylinders $(R - h/R + h = 0{\cdot}9,\ v = 0{\cdot}3)$

$L_x/(R+h)$	n	3-D [13]		M = 5		M = 8		M = 11		M = 14		M = 16	
		S	A	S	A	S	A	S	A	S	A	S	A
0·2	0a	1·6979	1·6481	1·6962	1·6462	1·6962	1·6462	1·6962	1·6462	1·6962	1·6462	1·6962	1·6462
	0t	15·708	7·8540	15·765	7·8562	15·708	7·8540	15·708	7·8540	15·708	7·8540	15·708	7·8540
	1	2·3932	1·6880	2·3960	1·6876	2·3960	1·6866	2·3960	1·6866	2·3960	1·6866	2·3960	1·6866
	2	0·13820	0·27690	0·13787	0·32423	0·13787	0·32224	0·13787	0·32224	0·13787	0·32224	0·13787	0·32224
	3	0·38830	0·82030	0·38711	0·87757	0·38708	0·87264	0·38708	0·87263	0·38708	0·87263	0·38708	0·87263
	4	0·73720	1·4786	0·73459	1·5399	0·73450	1·5310	0·73449	1·5310	0·73449	1·5310	0·73449	1·5310
	5	1·1769	2·1630	1·1721	2·2228	1·1719	2·2091	1·1719	2·2091	1·1719	2·2091	1·1719	2·2091
1	0a	1·6466	1·6906	1·6463	1·6890	1·6462	1·6890	1·6462	1·6890	1·6462	1·6890	1·6462	1·6890
	0t	3·1416	1·5708	3·1530	1·5712	3·1416	1·5708	3·1416	1·5708	3·1416	1·5708	3·1416	1·5708
	1	1·4845	1·2940	1·4887	1·2956	1·4859	1·2931	1·4857	1·2931	1·4857	1·2931	1·4857	1·2931
	2	0·14270	0·18520	0·14247	0·20263	0·14235	0·20097	0·14232	0·20068	0·14232	0·20055	0·14232	0·20055
	3	0·39990	0·46620	0·39918	0·47841	0·39871	0·47446	0·39859	0·47394	0·39857	0·47370	0·39857	0·47369
	4	0·75740	0·83250	0·75594	0·84264	0·75488	0·83599	0·75450	0·83521	0·75446	0·83483	0·75445	0·83481
	5	1·2067	1·2836	1·2040	1·2927	1·2021	1·2833	1·2013	1·2822	1·2013	1·2816	1·2012	1·2816
5	0a	0·50440	0·99040	0·50451	0·99376	0·50437	0·99040	0·50437	0·99039	0·50437	0·99039	0·50437	0·99039
	0t	0·62830	0·31420	0·63059	0·31425	0·62833	0·31416	0·62832	0·31416	0·62832	0·31416	0·62832	0·31416
	1	0·20180	0·43440	0·20328	0·52024	0·20212	0·43452	0·20211	0·43445	0·20211	0·43445	0·20211	0·43445
	2	0.14390	0·14580	0·14382	0·14709	0·14375	0·14683	0·14357	0·14659	0·14354	0·14644	0·14354	0·14642
	3	0·40320	0·40550	0·40264	0·40632	0·40240	0·40549	0·40195	0·40499	0·40185	0·40461	0·40181	0·40456
	4	0·76320	0·76530	0·76176	0·76562	0·76126	0·76417	0·76051	0·76336	0·76029	0·76270	0·76019	0·76257
	5	1·2148	1·2165	1·2118	1·2157	1·2111	1·2138	1·2100	1·2125	1·2096	1·2115	1·2094	1·2113

TABLE 4

Influence of the boundary conditions on the convergence rate of the frequency parameter $\bar{\omega}$ of certain cylindricla shells ($L_x/R = 5$, $h/R = 0{\cdot}05$, $n = 2$)

Boundary conditions	Model	Mode number	[0°/90°/0°] M				[0°/90°] M			
			8	11	14	16	8	11	14	16
CC	PARds	1st mode	108·05	107·91	107·82	107·81	105·59	105·54	105·49	105·48
		4th mode	459·21	457·33	457·01	456·83	405·99	404·67	404·49	404·42
	PARcs	1st mode	107·93	107·79	107·71	107·70	105·83	105·61	105·57	105·57
		4th mode	457·28	455·36	455·08	454·95	406·06	404·92	404·80	404·75
SS		1st mode	92·571	92·571	92·571	92·571	92·394	92·394	92·394	92·394
	PARds	4th mode	432·17	431·63	431·63	431·63	394·98	392·56	392·56	392·56
		1st mode	92·574	92·574	92·574	92·574	92·420	92·420	92·420	92·420
	PARcs	4th mode	431·38	430·82	430·82	430·82	394·88	392·45	392·45	392·45
FF		1st mode	26·557	26·557	26·557	26·557	40·985	40·985	40·985	40·985
	PARds	4th mode	286·13	285·93	285·88	285·88	270·76	270·68	270·64	270·64
		1st mode	26·575	26·575	26·575	26·575	41·057	41·057	41·057	41·057
	PARcs	4th mode	285·99	285·80	285·75	285·74	270·72	270·64	270·60	270·59
CF		1st mode	48·993	48·956	48·947	48·944	55·863	55·820	55·813	55·811
	PARds	4th mode	373·08	371·95	371·67	371·60	341·29	340·27	340·07	340·03
		1st mode	48·993	48·953	48·944	48·942	55·916	55·875	55·869	55·868
	PARcs	4th mode	372·32	371·18	370·91	370·85	341·26	340·30	340·15	340·12
CS		1st mode	98·933	98·801	98·756	98·743	97·775	97·627	97·594	97·585
	PARds	4th mode	445·76	444·48	444·16	444·07	399·70	398·65	398·48	398·44
		1st mode	98·882	98·741	98·698	98·688	97·805	97·672	97·648	97·643
	PARcs	4th mode	444·44	443·11	442·81	442·74	399·66	398·69	398·57	398·54
SF		1st mode	27·042	27·041	27·041	27·041	41·210	41·210	41·210	41·209
	PARds	4th mode	360·68	360·16	360·14	360·14	335·03	334·75	334·74	334·74
		1st mode	27·059	27·059	27·058	27·058	41·281	41·281	41·281	41·280
	PARcs	4th mode	360·31	359·80	359·78	359·78	334·95	334·68	334·66	334·66

Table 2 shows corresponding results obtained for three different values of M (namely, $M = 4$, 8 and 14), thus revealing further certain convergence aspect of the present approach.

An excellent agreement is observed between the corresponding numerical results that are compared in Table 2. For $M = 8$, in particular, the two approaches produce essentially identical numerical results. It is therefore concluded that, as far as CST approximation are concerned, the present approach is essentially equivalent to the one used in reference [12]. It is also of interest to note that the $M = 8$ and 14 terms truncations yield identical numerical results for SS shells but slightly different results for CC shells. This reveals that, as far as the SS shells are concerned, eight orthonormal polynomial terms in equations (3) predict the natural frequencies with an accuracy of five significant figures. In fact, even four polynomial terms yield frequencies with an accuracy of four significant figures. This, however, is not the case for CC shells for which, independently of the material arrangement, the convergence of the results is eventually slower. This observations makes therefore clear that changing the set of the edge boundary conditions affects the convergence rate of the numerical results.

For FF homogeneous isotropic cylinders ($v = 0{\cdot}3$) and several values of the circumferential wave number, n, Table 3 compares the lowest frequency parameters,

$$\hat{\omega} = \omega(R + h/2)\sqrt{(\rho/G)}, \tag{9}$$

based on the present parabolic shear deformable theory, with corresponding results obtained in reference [13] on the basic of a three-dimensional elasticity Ritz-type analysis. Since a three-dimensional elasticity analysis, although computationally more cumbersome, is always more accurate than a corresponding two-dimensional one, Table 3 may also be seen as part of an attempt to test the range of validity of the present shear deformable theory, at least as far as the isotropic materials are concerned. Moreover, the influence of some characteristics properties of the shell geometry on the rate of convergence of the present approach is also tested in Table 3, where numerical results obtained by changing M from five to 16 are also presented.

Most of the results presented in Table 3 on the basis of the present 2-D theory are in extremely good agreement with the corresponding 3-D predictions, which are assumed to be accurate up to four or five significant figures [13]. A smaller number of slightly inaccurate frequencies predicted by the present theory are not enough to change the very satisfactory picture of the comparisons performed in Table 3. As is further discussed at the end of this section, this is because these are frequencies of particularly short shells $[L_x/(R + h) = 0{\cdot}2]$ and may therefore be particularly influenced by the different sense (3-D or 2-D) in which the edge boundary conditions are applied in the two studies. Moreover, they are frequencies associated with antisymmetric vibration modes and, as such, are not among the lowest vibration shell frequencies, all of which were always in excellent agreement with their 3-D counterparts. As far as the rate of convergence is concerned, the present approach appears to converge slower when longer and therefore more flexible than shorter and therefore less flexible cylinders are considered. On an average, however,

an accuracy of three to four or four to five significant figures can be achieved when eight of 14 polynomial terms are, respectively, retained in equations (3).

The influence of the boundary conditions on the convergence rate of the present approach is next demonstrated in Table 4 where, for $n = 2$, the value of the first and the fourth frequency parameter,

$$\bar{\omega} = \frac{\omega L_x^2}{h}\sqrt{\rho/E_2}, \tag{10}$$

of certain two- and three-layered shells is tabulated as a function of the number M of the polynomial terms retained in equations (3). All the cylindrical shells involved in Table 4, as well as in the remaining tables and figures throughout this section, are assumed to have been made of a certain number of specially orthotropic layers, all of which have the following material properties:

$$E_1/E_2 = 25, \quad G_{12}/E_2 = G_{13}/E_2 = 0{\cdot}5; \quad G_{23}/E_2 = 0{\cdot}2, \quad \nu_{12} = 0{\cdot}25. \tag{11}$$

Upon considering the percentage difference between the corresponding frequencies predicted by using $M = 14$ and 16 polynomial terms, it can be easily verified that the fastest convergence rates are always associated with SS and FF shells. Moreover, a faster convergence is always achieved for an antisymmetric than a corresponding symmetric cross-ply lay-up whereas the convergence rate does not appear to be affected by whether the PARds or PARcs model is considered. With 14 polynomial terms being able to provide accurate results up to four or five significant figures, it was finally decided that $M = 14$ will be used in equations (3) for the predictions of all of the remaining results presented and discussed in this section. Moreover, all the results shown next were obtained on the basis of the PARcs model.

Tables 5–10 present the first four frequency parameters obtained for several values of the circumferential wave number, n, of certain three-layered symmetric and two-layered antisymmetric cross-ply laminated cylindrical shells subjected to six different sets of edge boundary conditions. It should be noted that, in all cases considered in Tables 5–10, the fundamental frequency occurs as the lowest frequency of the $n = 2$ mode, a fact that explains why this circumferential mode was chosen for the convergence tests performed in Table 4. Apart from the well-known trend [16, 17] according to which the fundamental vibration frequency of complete cylindrical shells is not necessarily associated with the lowest circumferential wave number, no other remarkable general trend can be drawn from the results shown in Tables 5–10. It is denoted, however, that for both the symmetric and the antisymmetric lay-up, the lowest fundamental frequency occurs for the FF cylinder (26·575 and 41·057, respectively), whereas the SF cylinder produces a slightly higher fundamental frequency (27·058 and 41·281 respectively). The manner in which the value of the fundamental frequencies is further increasing shows then that, regardless of the material arrangement, the order in which the boundary conditions can gradually increase the "global dynamic stiffness" of the shell is as follows: FF, SF, CF, SS, CS and CC.

At this point, it is of particular interest to report a similar trend that can be observed through the numerical results tabulated in reference [18]. These results

TABLE 5

First four frequency parameters, $\bar{\omega}$, for different values of n (CC, $L_x/R = 5$, $h/R = 0{\cdot}05$; PARcs)

	[0°/90°/0°]				[0°/90°]			
n	I	II	III	IV	I	II	III	IV
1	159·31	317·50	476·94	633·81	155·16	308·28	462·33	611·55
2	107·71	213·82	331·36	455·08	105·57	198·92	301·70	404·80
3	108·05	179·75	274·33	382·48	134·16	181·38	248·92	324·86
4	157·23	201·16	274·45	369·05	225·79	246·75	285·06	336·82
5	237·70	265·71	320·08	399·35	354·30	365·43	387·84	421·96
7	460·98	476·61	509·06	562·24	693·81	699·34	710·60	728·93
10	920·32	930·57	950·76	983·89	1373·2	1376·9	1383·80	1394·9

TABLE 6

First four frequency parameters, $\bar{\omega}$, for different values of n (SS, $L_x/R = 5$, $h/R = 0{\cdot}05$; PARcs)

	[0°/90°/0°]				[0°/90°]			
n	I	II	III	IV	I	II	III	IV
1	151·49	310·57	353·55	466·61	147·94	305·03	353·54	457·22
2	92·574	199·81	311·75	430·82	92·420	191·76	291·93	392·45
3	95·368	162·94	250·28	352·51	126·13	173·42	237·76	310·28
4	150·42	186·82	250·99	338·08	226·26	241·20	276·04	323·65
5	233·97	255·33	300·58	371·18	352·56	361·87	381·51	411·87
7	459·42	471·07	497·26	542·92	693·18	697·57	707·19	723·14
10	919·60	927·79	944·59	973·27	1373·0	1375·9	1381·9	1391·7

dealt with the free vibration and buckling under axial compression of certain [0°/90°/0°] and [0°/90°] cylindrical and spherical shallow shell panels having a rectangular plan form. Assuming that these panels have two opposite edges simply supported. Librescu *et al.* [18] applied to the partial differential equations of the shell theories employed the Levy approach in conjunction with the state space concept. Hence, using exact mathematical means, reference [18] tabulates free vibration and buckling results for plates and shallow shells having two opposite edges simply supported and the other two edges subjected to different sets of boundary conditions. Though not explicitly stated in reference [18], these results clearly show that, regardless of the material arrangement, the order in which the boundary conditions can gradually increase the "global dynamic stiffness" but also the corresponding "global buckling stiffness" of the structure is precisely the same. Namely: FF, SF, CF, SS, CS and CC.

TABLE 7

First four frequency parameters, $\bar{\omega}$, for different values of n (FF, $L_x/R = 5$, $h/R = 0{\cdot}05$; PARcs)

	[0°/90°/0°]				[0°/90°]			
n	I	II	III	IV	I	II	III	IV
1	304·13	338·10	485·88	612·92	297·23	335·49	479·71	599·56
2	26.575	28·418	185·42	285·75	41·057	41·931	176·74	270·60
3	74·905	77·008	145·75	226·52	115·25	116·32	160·27	222·35
4	142·93	145·14	174·08	230·31	219·17	220·30	234·81	266·54
5	229·74	231·97	247·62	285·05	351·05	352·14	359·14	376·35
7	456·60	458·78	467·98	489·35	692·18	693·14	697·03	705·58
10	917·18	919·22	926·46	941·08	1372·1	1372·9	1375·8	1381·5

TABLE 8

First four frequency parameters, $\bar{\omega}$, for different values of n (CC, $L_x/R = 5$, $h/R = 0{\cdot}05$; PARcs)

	[0°/90°/0°]				[0°/90°]			
n	I	II	III	IV	I	II	III	IV
1	74·326	224·19	388·86	541·98	71·692	216·15	378·72	524·89
2	48·944	137·16	255·64	370·91	55·869	130·50	239·19	340·15
3	79·329	120·96	205·15	300·35	117·66	142·01	202·58	272·50
4	144·50	163·33	216·16	292·52	220·01	228·72	256·38	298·49
5	230·72	241·80	275·29	333·42	351·53	356·16	370·59	395·88
7	457·31	464·19	482·77	518·34	692·48	695·20	702·26	715·18
10	917·79	923·10	935·60	958·22	1372·3	1374·4	1379·0	1387·1

For certain [0°/90°/0°] and [0°/90°] shells having FF, SS and CC edges, Tables 11–13 show the influence of the L_x/R ratio on the first and the fourth frequency parameters, $\bar{\omega}$, obtained for $n = 4$ and 10. These results are based on the the PARcs model and, apart from their individual merit and interest, they are further used for the plots drawn in Figs. 2–4. For the results tabulated in Tables 11–13, Figures 2–4, respectively, show the percentage difference,

$$\Delta\omega(\mathrm{I})\% = [\bar{\omega}\,(I)_{\mathrm{PARds}} - \bar{\omega}\,(\mathrm{I})_{\mathrm{PARcs}}] \cdot 100/\bar{\omega}\,(\mathrm{I})_{\mathrm{PARcs}} \tag{12}$$

of the corresponding frequency parameters that are based on the PARds and PARcs models. The form of equation (12) makes clear that the positive (negative) percentage differences reveal that the PARds model predicts higher (lower) frequencies than the PARcs model does. It should be also mentioned, however, that

TABLE 9

First four frequency parameters, $\bar{\omega}$, for different values of n (CS, $L_x/R = 5$, $h/R = 0{\cdot}05$; PARcs)

	[0°/90°/0°]				[0°/90°]			
n	I	II	III	IV	I	II	III	IV
1	153·77	314·02	471·65	627·02	149·60	306·67	459·62	608·05
2	98·698	206·81	321·31	442·81	97·648	195·50	296·65	398·57
3	100·95	171·24	261·97	367·30	129·68	177·52	243·17	317·45
4	153·40	193·73	262·32	353·31	223·83	243·99	280·39	330·06
5	235·59	260·22	309·91	384·95	353·33	363·62	384·55	416·74
7	460·10	473·64	502·86	552·27	693·46	698·42	708·82	725·92
10	919·93	929·09	947·53	978·40	1373·1	1376·4	1382·8	1393·3

TABLE 10

First four frequency parameters, $\bar{\omega}$, for different values of n (SF, $L_x/R = 5$, $h/R = 0{\cdot}05$; PARcs)

	[0°/90°/0°]				[0°/90°]			
n	I	II	III	IV	I	II	III	IV
1	211·13	337·13	405·63	544·39	206·48	334·04	400·64	535·48
2	27·058	132·30	244·94	359·78	41·281	128·28	232·86	334·66
3	75·441	115·64	194·46	287·77	115·51	139·20	197·16	266·61
4	143·49	159·51	207·22	279·99	219·42	226·97	252·76	293·45
5	230·31	239·34	268·78	322·66	351·28	355·12	368·32	392·22
7	457·16	462·92	479·24	511·56	692·40	694·70	701·12	713·14
10	917·72	922·43	933·73	954·54	1372·3	1374·1	1378·4	1386·0

unlike the present situation, the requirement of the continuous interlaminar stresses becomes essentially immaterial when the transverse shear moduli that correspond to consecutive layers do not differ considerably. As a matter of f act, the PARds and PARcs model become essentially equivalent when the ratio of these moduli approaches 1 (see also reference [19]).

Figure 2 reveals that, for either [0°/90°/0°] or [0°/90°] shells having FF edges, the PARds model always produces lower vibrations frequencies whereas the percentage difference between the PARds and the PARcs frequencies are essentially independent of the L_x/R ratio. Moreover, these percentage differences are higher for the antisymmetric cross-ply lay-up whereas they are increasing with increasing the circumferential wave number. Figures 3 and 4 make evident that these observations still apply to relatively long and to long shells ($L_x/R > 2$) having SS

TABLE 11

First and four frequency parameters, $\bar{\omega}$, for different L_x/R ratios (FF, h/R = 0·05; PARcs)

	[0°/90°/0°]				[0°/90°]			
	I		IV		I		IV	
L_x/R	$n = 4$	$n = 10$	$n = 4$	$n = 10$	$n = 4$	$n = 10$	$n = 4$	$n = 10$
0·2	0·22857	1·4668	9·9023	13·270	0·35058	2·1946	10·675	10·936
0·4	0·91429	5·8673	20·987	21·870	1·4024	8·7788	14·456	21·343
0·6	2·0572	13·202	26·794	48·321	3·1555	19·753	19·871	41·618
0·8	3·6575	23·472	34·380	64·049	5·6099	35·118	33·836	55·119
1	5·7152	36·676	53·317	78·144	8·7657	54·873	45·273	72·863
1.5	12·861	82·530	85·785	121·23	19·724	123·47	62·836	138·14
2	22·865	146·73	103·00	181·26	35·065	219·51	81·92	232·42
2·5	35·729	229·27	120·15	260·46	54·790	342·99	103·86	354·82
3	51·451	330·17	138·47	358·91	78·898	493·92	128·99	505·00
4	91·473	586·98	180·23	612·65	140·27	878·11	189·95	888·21
5	142·93	917·18	230·31	941·08	219·17	1372·1	266·54	1381·5
6	205·82	1320·8	289·96	1343·5	315·61	1975·8	359·79	1984·8
7	280·15	1797·7	360·07	1819·8	429·59	2689·3	470·29	2698.0
8	365·92	2348·1	441·23	2369·6	561·10	3512·6	598·39	3521·0
9	463·12	2971·8	533·83	2992·9	710·15	4445·6	744·23	4453·8
10	571·76	3668·9	638·08	3689·8	876·75	5488·4	907·89	5496·5

and CC boundaries respectively. For short shells, however, the edge boundary conditions come into play and although they have a relatively moderate effect for SS shells (Figure 3), they affect these differences dramatically for CC shells (Figure 4). It is of interest to notice in this respect that, although the differences shown in Figure 3 for SS shells are always kept within acceptable engineering limits (less than 5%), they became as high as -11 or -18% for very short CC shells having a [0°/90°/0°] or [0°/90°] lay-up respectively (Figure 4). It should not be ignored on the other hand, that is such cases of very short shells in which two-dimensional shell theories either neglect or grossly approximate some of the boundary-layer edge effects, the accuracy of the present two-dimensional shell theory may become questionable. For the accurate dynamic analysis of short or even relatively long laminated composite shells subjected to different sets of boundary conditions, the modelling of the interlaminar stress distribution may becomes a serious issue for further investigation, as already is for the stress analysis of such elements (see, for instance, references [20–23]).

There are also, however, cases of edge boundary conditions in which, despite the particularly small axial length of the shell, two-dimensional shear deformable theoreies have produce free vibration results that are in very good agreement with the corresponding results based on the exact three-dimensional elasticity analyses. Apart from most but not all of the relevant results presented in Table 3 for FF

TABLE 12

First four frequency parameters, $\bar{\omega}$, for different L_x/R ratios (SS, h/R = 0·05; PARcs)

	[0°/90°/0°]				[0°/90°]			
	I		IV		I		IV	
L_x/R	$n = 4$	$n = 10$	$n = 4$	$n = 10$	$n = 4$	$n = 10$	$n = 4$	$n = 10$
0·2	2·2627	5·6569	15·421	25·654	2·2616	5·6383	15·328	25·355
0·4	9·0510	11·578	41·433	41·780	7·2294	11·253	39·870	40·632
0·6	12·884	18·430	55·252	56·571	9·3674	21·595	47·780	51·374
0·8	15·326	28·011	68·249	90·510	12·039	36·656	53·875	90·213
1	17·771	40·667	79·928	120·8	15·295	56·242	59·442	107·36
1.5	24·991	85·741	127·28	173·83	26·153	124·63	111·87	164·92
2	34·524	149·59	184·77	235·41	41·099	220·57	131·82	253·05
2·5	46·705	231·95	211·21	311·45	60·300	343·99	154·73	371·61
3	61·670	332·73	235·63	405·31	83·851	494·88	181·07	519·38
4	100·22	589·45	284·34	650·67	144·19	879·03	244·73	899·88
5	150·42	919·60	338·08	973·27	222·26	1373·0	323·65	1391·7
6	212·32	1323·2	399·85	1371·9	318·08	1976·7	418·45	1994·1
7	285·88	1800·1	471·04	1845·4	431·59	2690·2	529·64	2706·6
8	371·05	2350·5	552·39	2393·4	562·76	3513·5	657·58	3529·1
9	467·80	2974·2	644·36	3015·4	711·56	4446·6	802·56	4461·5
10	576·08	3671·3	747·27	3711·1	877·95	5489·4	964·80	5503·9

TABLE 13

First four frequency parameter, $\bar{\omega}$, for different L_x/R ratios (CC, h/R = 0·05; PARcs)

	[0°/90°/0°]				[0°/90°]			
	I		IV		I		IV	
L_x/R	$n = 4$	$n = 10$	$n = 4$	$n = 10$	$n = 4$	$n = 10$	$n = 4$	$n = 10$
0·2	8·6127	8·7420	20·782	29·929	8·7128	8·9679	21·600	28·431
0·4	13·485	14·612	47·888	70·673	12·023	14·746	51·114	69·844
0·6	18·020	22·156	88·003	88·919	14·414	24·170	85·296	87·247
0·8	21·997	31·910	106·50	108·74	16·876	38·490	97·612	103·16
1	25·557	44·358	124·62	129·35	19·801	57·617	107·68	120·00
1.5	33·931	88·519	165·93	184·40	29·953	125·47	128·66	176·55
2	43·375	151·65	201·29	248·10	44·554	221·19	149·01	262·26
2·5	55·113	233·55	232·16	325·31	63·658	344·49	171·50	378·80
3	69·629	334·02	260·23	419·29	87·231	495·31	197·13	525·15
4	107·50	590·37	313·53	663·21	147·68	879·36	259·22	903·95
5	157·23	920·32	369·05	983·89	225·79	1373·2	336·82	1394·9
6	218·70	1323·7	431·00	1380·8	321·52	1976·9	430·67	1996·7
7	291·84	1800·6	501·60	1853·1	434·86	2690·4	541·25	2708·9
8	376·59	2350·9	582·07	2400·1	565·82	3513·7	668·86	3531·1
9	472·91	2974.6	673.12	3021.2	714.37	4446.7	813·74	4463·4
10	580·79	3671·7	775·16	3716·4	880·53	5489·5	976·03	5505·6

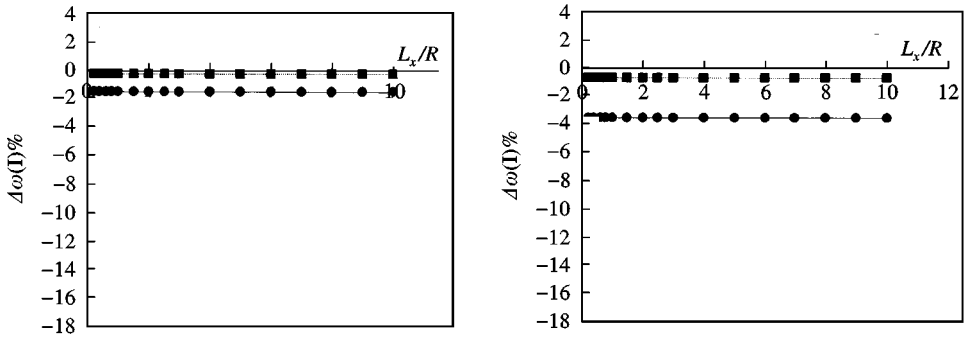

Figure 2. Percentage difference between PARds and PARcs models through L_x/R ratio with completely free boundary conditions. (■ $n = 4$ —●— $n = 10$ [0°/90°/0°]: FF) (■ $n = 4$ —●— $n = 10$ [0°/90°]: FF).

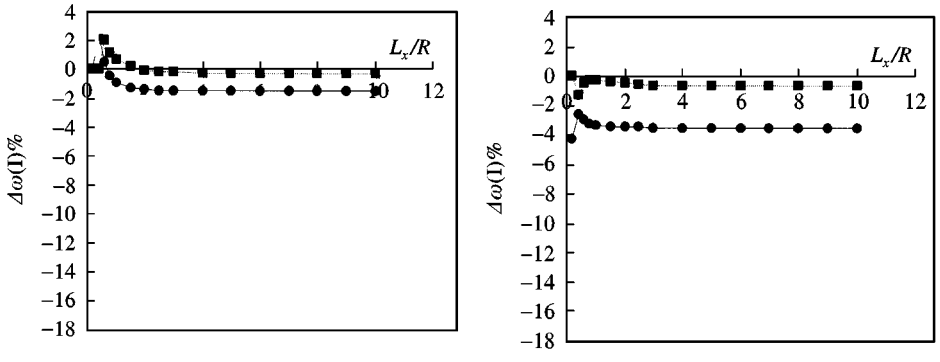

Figure 3. Percentage difference between PARds and PARcs models through L_x/R ratio with simply supported boundary conditions. (■ $n = 4$ —●— $n = 10$ [0°/90°/0°]: SS) (■ $n = 4$ —●— $n = 10$ [0°/90°]: SS).

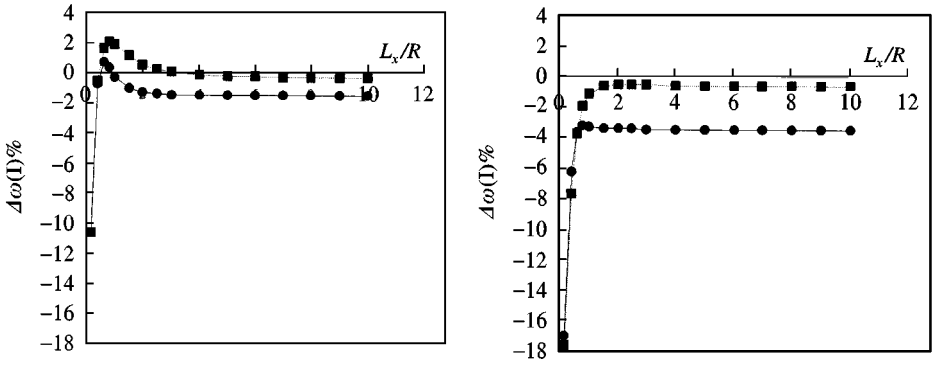

Figure 4. Percentage difference between PARds and PARcs models through L_x/R ratio with clamped boundary conditions. (■ $n = 4$ —●— $n = 10$ [0°/90°/0°]: CC) (■ $n = 4$ —●— $n = 10$ [0°/90°]: CC).

shells, short cylindrical shells having both their edges simply suppoprted are definitely included in this category [5, 24]. It is worth mentioning in this connection that, when dealing with a family of particularly short SS shells and using $M = 8$, the present approach predicted identical vibration frequencies to those tabulated in Table 2 of reference [5] for either the PARcs or PARds model. These frequencies [5] were obtained on the basis of the state space concept and, as already mentioned, were found to be in very good agreement with the corresponding results based on an exact three-dimensional elasticity analysis [25].

4. CONCLUSIONS

This paper extended the applicability of the Ritz-type procedure presented in reference [1], towards an advanced study of the influence of the edge boundary conditions on the vibration characteristics of complete cross-ply laminated cylindrical shells. This analysis was based on the conjunction of the Ritz method with appropriate, complete bases of orthonormal polynomials and its subsequent application on the energy functional of the Love-type version of a unified shear-deformable shell theory. As a result, two different kinds of shear deformable Love-type shell modes were employed, including versions that either fulfil (PARcs) or violate (PARds) the continuity of the interlaminar stresses along the shell thickness. Both models are, however, based on a well-known polynomial form of the shape functions, which is given according to equations (2).

As far as the performance of the method is concerned, an excellent agreement was observed with corresponding numerical results obtained in reference [12] on the basis of a classical shell theory. Moreover, a very good agreement was observed with a rather limited number of existing relevant results that were obtained in references [5, 13, 25] on the basis of more accurate, but computationally more cumbersome, three-dimensional elasticity analyses. It should be noted in this respect, that reference [13] dealt with homogeneous isotropic cylindical shells having both their edges free of traction whereas the three-dimensional elasticity results presented in references [5, 25] were for a family of very short cross-ply laminated cylindrical shells having both their edges simply supported.

As far as the modelling is concerned, particular emphasis was given to the version of the parabolic shear deformable shell theory that considers continuity of the interlaminar stresses. Moreover, the relation of this version of the theory as well as its performance with respecdt to the corresponding older version that violates this continuity requirement [8] was further investigated. It was concluded, in this respect, that the accurate modelling of the interlaminar stress distribution may become a serious issue for further investigation, particularly for short shells.'

ACKNOWLEDGMENTS

The work reported in this paper is part of a European Joint Project Grant that was awarded to the authors by the Royal Society of London. The authors wish to acknowledge the anonymous reviewers of reference [1], whose interesting

comments created motivation for a part of the present paper. The constructive comments of the reviewers of the present paper are also acknowledged.

REFERENCES

1. K. P. Soldatos and A. Messina 1998 *Journal of Sound and Vibration* **218**, 219–243. Vibration studies of cross-ply laminted shear deformable circular cylinders on the basis of orthogonal polynomials.
2. K. P. Soldatos and T. Timarci 1993 *Composite Structures* **25**, 165–171. A unified formulation of laminated composite, shear deformable, five-degrees-of-freedom cylindrical shell theories.
3. I. A. Jones, E. J. Williams and A. Messina 1996 *Proceedings of 2nd International Conference on Structural Dynamics Modelling, NAFEM*, 267–279. Cumbria. Theoretical, experimental and finite element modelling of laminated composite shells.
4. A. A Khdeir and J. N. Reddy 1990 *Computers and Structures* **34**, 817–826. Influence of edge conditions on the modal characteristics of cross-ply laminated shells.
5. T. Timarci and K. P. Soldatos 1995 *Journal of Sound and Vibration* **187**, 609–624. Comparative dynamic studies for symmetric cross-ply circular cylindrical shells on the basis of a unified shear deformable shell theory.
6. A. Messina and K. P. Soldatos 1999 *International Journal of Mechanical Sciences* **41**, 891–918. Vibration of completely free composite plates and cylindrical shell panels by a higher order theory.
7. A. Messina and K. P. Soldatos 1999 *Journal of Acoustical Society of America* Influence of edge boundary conditions on the free vibration of cross-ply laminated circular cylindrical panels (in press).
8. J. N. Reddy and C. F. Liu 1985 *International Journal of Engineering Sciences* **23**, 319–330. A higher-order shear deformation theory of laminated elastic shells.
9. R. M. Jones 1975 *Mechanics of Composite Materials*. New York: Hemisphere.
10. R. B. Bhat 1985 *Journal of Sound and Vibration* **102**, 493–499. Natural frequencies of rectangular plates using characteristic orthogonal polynomials in Rayleigh–Ritz method.
11. S. M. Dickinson and A. Di-Blasio 1986 *Journal of Sound and Vibration* **108**, 51–62. On the use of orthogonal polynomials in the Rayleigh–Ritz method for the study of the flexural vibration and buckling of isotropic and orthotropic rectangular plates.
12. Y. Narita, Y. Ohta, G. Yamada and Y. Kobayashi 1992 *American Institute of Aeronautics and Astronautics Journal* **30**, 790–796. Analytical method for vibration of angle-ply cylindrical shells having arbitrary edges.
13. J. So and A. W. Leissa 1997 *Journal of Vibrtaion and Acoustics* **119**, 89–85. Free vibrations of thick hallow circular cylinders from three-dimensional analysis.
14. M. E. Vanderpool and C. W. Bert 1981 *American Institute of Aeronautics and Astronautics Journal* **19**, 634–641. Vibration of a materially monoclinic, thick-wall circular cylindrical shell.
15. K. P. Soldatos 1991 *Journal of Sound and Vibration* **144**, 109–129. A refined laminated plate and shell theory with applications.
16. R. N. Arnold and G. B. Warburton 1949 *Proceedings of the Royal Society of London, Series A* **197**, 238–256. Flexural vibrations of the wall of thin cylindrical shells having feely supported ends.
17. H. Kraus 1967 *Thin Elastic Shells*. London and New York: Wiley.
18. L. Librescu, A. A. Khdeir and D. Frederick 1989 *Acta Mechanica* **76**, 1–33. A shear deformable theory of laminated composite shallow shell-type panels and their response analysis I: free vibration and buckling.
19. L. Librescu and W. Lin 1996 *European Journal of Mechanics, A/Solids* **16**, 1095–1120. Two models of shear deformable laminted plates and shells and their use in prediction of global response behavior.

20. K. P. Soldatos, and P. Watson 1997 *Acta Mechanica* **123**, 163–186. A method for improving the stress analysis performance of two-dimensional theories for composite laminates.
21. K. P. Soldatos and P. Watson 1997 *International Journal of Solids and Structures* **34**, 2857–2885. A general four-degrees-of-freedom theory suitable for the accurate stress analysis of homogeneous and laminated composites beams.
22. K. P. Soldatos and P. Watson 1997 *Mathematics and Mechanics of Solids* **2**, 459–489. Accurate stress analysis of laminated plates combining a two-dimensional theory with the exact three-dimensional solution for simply supported edges.
23. X. Shu and K. P. Soldatos, *International Journal of Solids and Structures*. Cylindrical bending of angle-ply laminated subjected to different sets of edge boundary conditions. (accepted).
24. M. Disciuva and E. Carrera 1992 *Journal of Applied Mechanics* **59**, 222–224. Elastodynamic behaviour of relatively thick, symmetrically laminated, anisotropic circular cylindrical shells.
25. J. Q. Ye and K. P. Soldatos 1994 *Composites Engineering* **4**, 429–444. Three-dimensional vibrations of laminated cylinders and cylindrical panels with a symmetric or an antisymmetric cross-ply lay-up.